REGULAR PAPER

Manufacturing of magnesium/aluminum bimetallic ring components by friction stir assisted simultaneous forging and solid-state joining

Mounarik Mondal[1] · Soumyabrata Basak[1] · Hrishikesh Das[2] · Sung-Tae Hong[1] · Howook Choi[3] · Ju-Won Park[3] · Heung Nam Han[3]

Abstract

A bimetallic ring component is forged by a friction stir assisted forging (FS-forging). A cylindrical bimetallic blank, magnesium AZ31 cylinder (Mg core) tightly fitted inside an aluminum 6061-T6 tube (Al skin), is used. In the FS-forging, the frictional heat and stirring of rotating tool forge the blank into a desired shape, while simultaneously generate a solid-state joint between the Mg core and the Al skin, without additional external heating, as confirmed by the microstructural analysis and mechanical tests. The microstructural analysis also shows that the characteristics of the solid-state joint can be different depending on the process parameters.

Keywords Forging · Solid-state joining · Intermetallics · friction stir welding

1 Introduction

The use of bimetallic structural components to minimize issues from using a single material has drawn interest from industries. However, with conventional processes, researchers have reported complications in the manufacture of such bimetallic components, generally due to the dissimilar mechanical/material properties of the selected metal alloys [1].

In the manufacture of bimetallic materials or components, a simultaneous forming and joining is frequently considered. Bae et al. [2] cladded magnesium (Mg) and aluminum (Al) alloys using twin roll casting and reported the formation of $Mg_{17}Al_{12}$ intermetallic layer resulting strong bonding. Golovko et al. [3] performed hot extrusion of an Al–Mg bimetallic rod for simultaneous forming and joining with the help of furnace heating. Ng et al. [4] successfully performed electrically assisted roll bonding of ultra-thin Al alloy sheets with the same alloy or Cu alloy sheets at a relatively low bonding load and achieved higher bonding strength as compared to the conventional process. Recently, Napierala et al. [5] proposed draw forging for simultaneous cold forming and joining of Al alloy and steel to manufacture multi-material component.

Friction stir welding (FSW) is an effective solid-state joining technique for nonferrous dissimilar materials. During FSW, frictional heat and severe straining by a rotating tool are applied to the workpiece material, which induce dynamic recrystallization, and consequently fine microstructures inside the material. The unique characteristics of FSW can be effectively used to manufacture bimetallic structural components, as suggested in friction stir extrusion of bimetallic Al/Fe blanks [6]. Compared with other forming processes, such as roll bonding, cladding, and extrusion, used for fabricating bimetallic components, approaches based on friction stirring remove or minimize the need for external heating, thus reducing both the energy requirement and the production time [7, 8].

Ring components are finding increasing applications in many industries as rotary machine components or connecting components due to recent developments in ring forming processes, such as incremental ring rolling [9], orbital forging [10], and spinning [11]. Cleaver et al. [12] successfully demonstrated that ring components with variable wall

✉ Sung-Tae Hong
  sthong@ulsan.ac.kr

1 School of Mechanical Engineering, University of Ulsan, Ulsan, South Korea

2 Applied Materials and Manufacturing Group, Pacific Northwest National Laboratory, Richland, WA, USA

3 Department of Materials Science and Engineering and Research Institute of Advanced Materials, Seoul National University, Seoul, Republic of Korea

thickness can be formed by a ring rolling technique. Traditionally, most metallic ring components are manufactured using a single material.

The high specific strength and low density of Mg alloys can make them candidates for structural components, including ring components. However, the limitations of the material properties, including poor formability, brittleness at room temperature, and low corrosion resistance, hinder the use of those alloys in practical applications. To counter the limits of Mg alloys for structural components, the concept of bimetallic components can be considered.

With their low density and good chemical compatibility with Mg alloys, Al alloys can be candidates to compose light-weight bimetallic combinations with Mg alloys. By properly combining Al alloys with Mg alloys, it is expected that the relatively high ductility and good corrosion resistance of Al alloys can minimize the issues from the material properties of Mg alloys [13, 14]. However, a simultaneous forming and joining of such bimetallic combinations generally requires external heating or preheating of the materials, mostly due to the limited formability of Mg alloys at room temperature. Naturally, the simultaneous forming and joining with external heating or preheating increases the production cost and consumes longer time.

In the present study, a friction stirring based approach to simultaneously forge and join a bimetallic ring component [15] is suggested. The friction stir assisted forging (simply, FS-forging) can eliminate the need for external heating or preheating for materials with a limited formability at room temperature (such as Mg alloys). The FS-forging is also expected to generate a dynamically recrystallized fine microstructure inside the forged component by friction stirring. Reported here is the demonstration of the feasibility of FS-forging by fabricating Mg/Al bimetallic ring components.

2 Experimental setup

Cylindrical rods of Al 6061-T6 and Mg AZ31b alloys (chemical compositions in Table 1), were used. For FS-forging, bimetallic blanks of the Al and Mg alloys were prepared, as schematically described in Fig. 1a. The Al rods were machined to cylindrical tubes (the Al skin) with an inner diameter of 10 mm, a wall thickness of 3 mm, and a height of 14 mm. Then the Mg rods, which were machined to solid cylinders (the Mg core) with a diameter of 10 mm and a height of 14 mm, were tightly fitted into the Al skins. A cylindrical FS-forging tool with a two-step shoulder and a die with a cylindrical cavity were designed, as described in Fig. 1b.

As described in Fig. 2a–d, FS-forging was conducted by plunging the rotating tool and the cylindrical bimetallic

Table 1 Alloying elements of AZ31B and Al6061-T6 (wt.%)

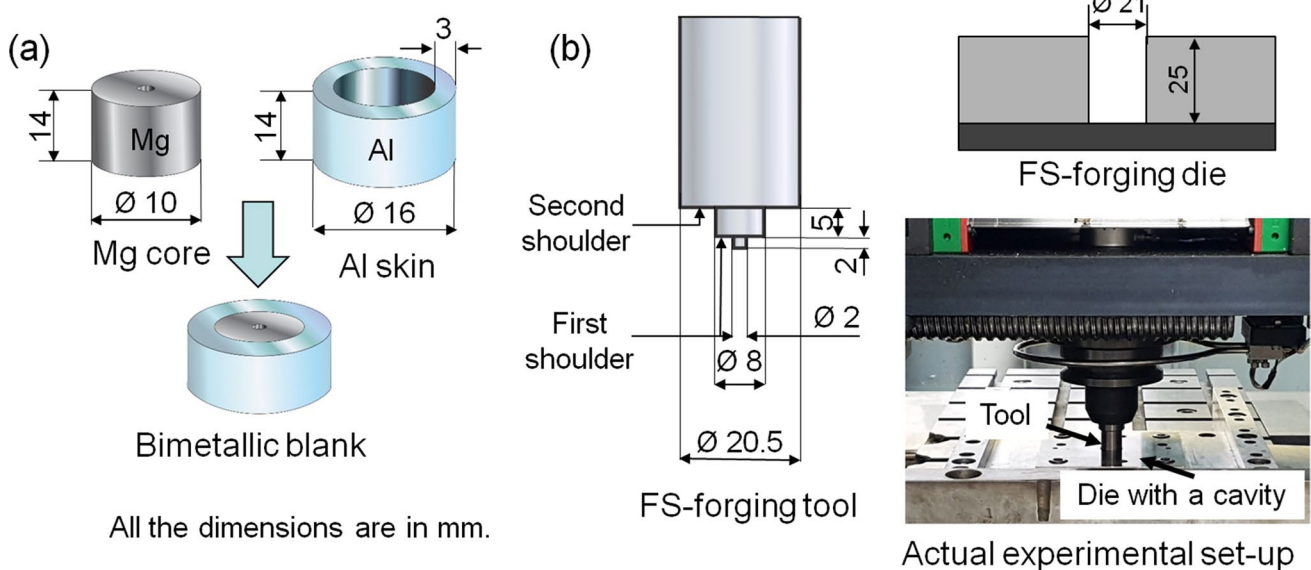| Materials	Mg	Al	Zn	Ca	Cr	Mn	Si	Ti	Cu	Fe
AZ31B	Bal	2.5	0.60	0.040	–	0.20	0.10	–	0.05	0.005
Al6061-T6	1.2	Bal	0.25	–	0.25	0.14	0.40	0.15	0.15	0.70

Fig. 1 **a** A schematic of a Mg/Al bimetallic blank, **b** a cylindrical FS-forging tool with a two-step shoulder and a die with a cylindrical cavity
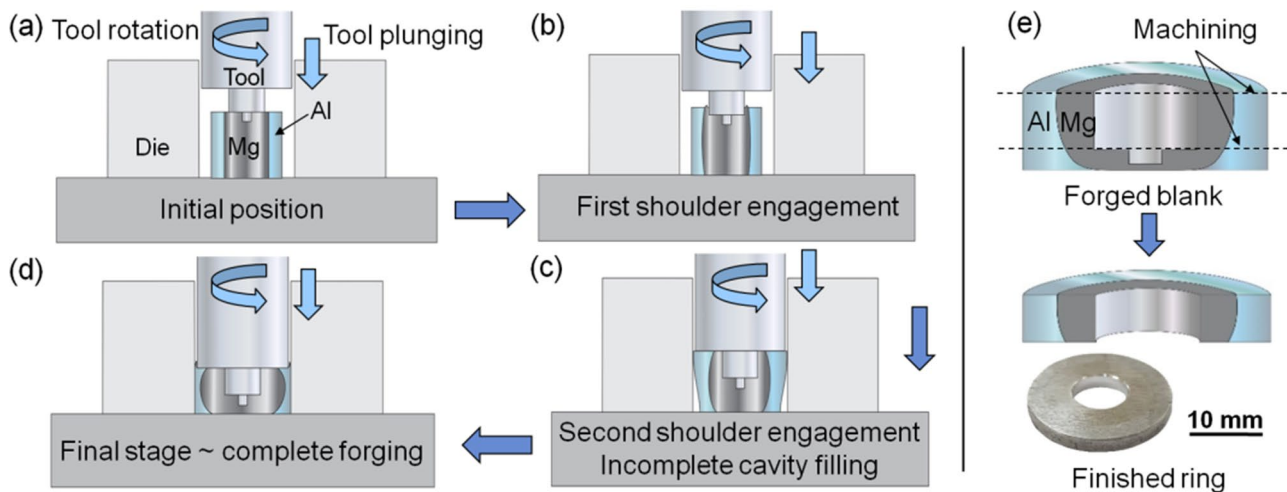
Fig. 2 **a–d** FS-forging stages, **e** a forged blank and a bimetallic ring

Table 2 FS-forging parameters

Parameter set	Tool rotational speed (rpm)	Tool plunging speed (mm/min)	Dwell time (s)
1	1400	10	05
2			08

blank into the die cavity using a custom-made FSW machine (RM1A, MTI, USA) with the forging parameters listed in Table 2. The tool rotational speed and the plunging speed were selected based on the results of a separately conducted preliminary experiment. In the preliminary experiment, total twenty four different sets of parameters were considered with six different tool rotation speeds varying from 600–1600 rpm (with an increase of 200 rpm) and four different plunging speeds ranging from 4–10 mm/min (with an increase of 2 mm/min) to select the combination of the tool rotation speed and plunging speed in Table 2. Other sets of parameters resulted in either softening of Mg core or excessive increase of forging force. The failed results of the preliminary experiment will not be further discussed in the present study since the failures were mostly due to insufficient or excessive energy input. With the selected combination of the tool rotation speed and plunging speed, two different dwell times were considered to see the effect of dwell time on diffusion, which is the core mechanism of solid-state joining between the Mg core and Al skin. Since the rotating FS-forging tool also served as an upper die during forging, the FS-forging became a closed die forging with a flash along the gap between the tool and the die cavity. After FS-forging, the top (2 mm) and bottom (3 mm) portions of a forged blank was machined (Fig. 2e) to complete a bimetallic

ring component with an approximate height of 3 mm (an outer diameter of 21 mm and an inner diameter of 8 mm).

After the FS-forging, cross-sections were prepared along the tool plunging direction (the height direction of a ring) for microstructural analysis. The cross-section of a forged blank was first examined by optical microscopy (OM, A1m Axio Imager, Carl Zeiss, Germany) to observe any macroscopic defects. Then, energy dispersive X-ray spectroscopy and electron backscatter diffraction (EBSD) analysis were conducted on the cross-sections of bimetallic rings. A field emission scanning electron microscope (FE-SEM, SU70, Hitachi, Japan) equipped with an EBSD system (Hikari EBSD detector with the TSL OIM 6.1 software, Hitachi, Japan) was used. A standard metallographic grinding technique for polishing, combined with an ethanol-based diamond paste to avoid oxidation of the Mg core, was used. For the EBSD analysis, the cross sections of bimetallic rings were further polished using colloidal silica. The accelerating voltage of 15 kV and the working distance of 15 mm were used in the EBSD analysis. A critical misorientation angle of 15° was taken for grain identification. The mechanical properties of the bimetallic rings were evaluated by microhardness measurement. A Vickers microhardness tester (Mitutoyo hardness testing machine, Mitutoyo, Japan) was used (a load of 0.49 N for 10 s).

3 Results and discussions

At the initiation of the FS-forging, the interaction of the cold blank with the die at the bottom and the tool on the top resulted in steep rises in the axial force (the forging force) and the torque response. After the initial peak, the axial force and torque showed approximate plateaus until

the engagement of second shoulder (Fig. 3). As the second shoulder began to engage the blank, the axial force steadily increased until it rapidly increased upon the completion of forging. Due to the frictional heat and heat dissipation from plastic deformation, the temperature of the blank increased rapidly and softened the both Mg and Al alloys. Temperature measurement using a separately prepared die (with a hole at center of the cavity to connect a k-type thermocouple to a deforming blank) suggests that the temperature of the blank exceeded 400 °C during forging, while a precise measurement was difficult due to the severe plastic deformation of the blank. Due to the use of the two-step shoulder tool, the axial force steadily increased as the second shoulder contacted the blank (marked in Fig. 3). Once the second shoulder fully contacted the bimetallic blank, the axial force showed a second plateau until the occurrence of a sharp increase with the completion of forging.

To understand the deformation behavior of the bimetallic blank during FS-forging, forging was interrupted at various compressive displacements (marked as I to VI in Fig. 3) and the blank was removed from the forging die, as shown in Fig. 4a with cross sections. As the first shoulder of the rotating tool began to engage the Mg core of the bimetallic blank (stage I), the Mg core softened quickly by frictional heat and plastic heat dissipation. Since the diameter of the first shoulder was slightly smaller than that of the Mg core, the Mg core was slightly backward extruded against the Al skin (stage II). Until the contact of the second shoulder to the blank, the rotating tool plunged into the heated Mg core with a small amount of deformation of the Al skin (stage III). As the second shoulder began to engage the deforming blank, the backward extruded Mg core was compressed, and the entire blank began to deform (stage IV).

As clearly indicated by the diameters of top and bottom surfaces of deforming blank at each stage (Fig. 4b), the deformation of the blank was not symmetric with respect to the middle height of the blank since the generation of frictional heat and the relative motion between the rotating tool and the deforming blank mostly occurred at the top surface of the blank. With the asymmetric deformation, the upper region of the deforming blank contacted the die wall, while the lower region of the deforming blank still expanded in the radial direction to fill the remaining die cavity (stage V). The height of the blank continuously decreased until the blank was completely forged into the desired shape (stage VI) with a steep increase in the axial force. A small amount of flash formation was observed through the clearance between the tool and the cylindrical cavity.

The result of OM shows that the bimetallic blank was successfully forged without macroscopic defects into the shape of a closed cavity, which consisted of the shoulder of the rotating tool and the cylindrical cavity of the stationary lower die (Fig. 5). A noticeable barreling of the Mg core was observed in the cross section of the forged blank, which corresponds to high friction between the rotating tool/bottom of the die cavity and the top/bottom surfaces of the blank. The OM also suggests development of a thick intermetallic region at the Mg/Al interface, as marked in the Fig. 5. This typically occurred for the parameter set of 1400/5. While the thick intermetallic region was frequently observed through the analysis of the results with the parameter set of 1400/5, its location and size were random. For the parameter set of 1400/8, a relatively thick intermetallic layer evenly developed along the entire interface. After FS-forging, the top and bottom surfaces of a forged bimetallic blank were machined (along the white lines in Fig. 5) to a bimetallic ring component.

The results of FE-SEM analysis across the Mg/Al interface on the cross sections of the final ring components shown in Fig. 6a reveal that the Mg core and the Al skin were successfully metallurgically joined by the formation of intermetallic layer, which was aided by diffusion
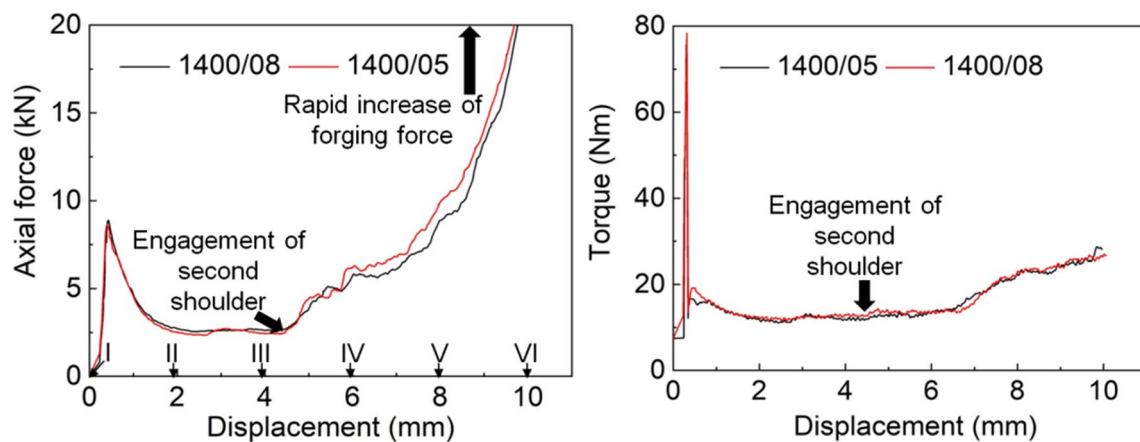

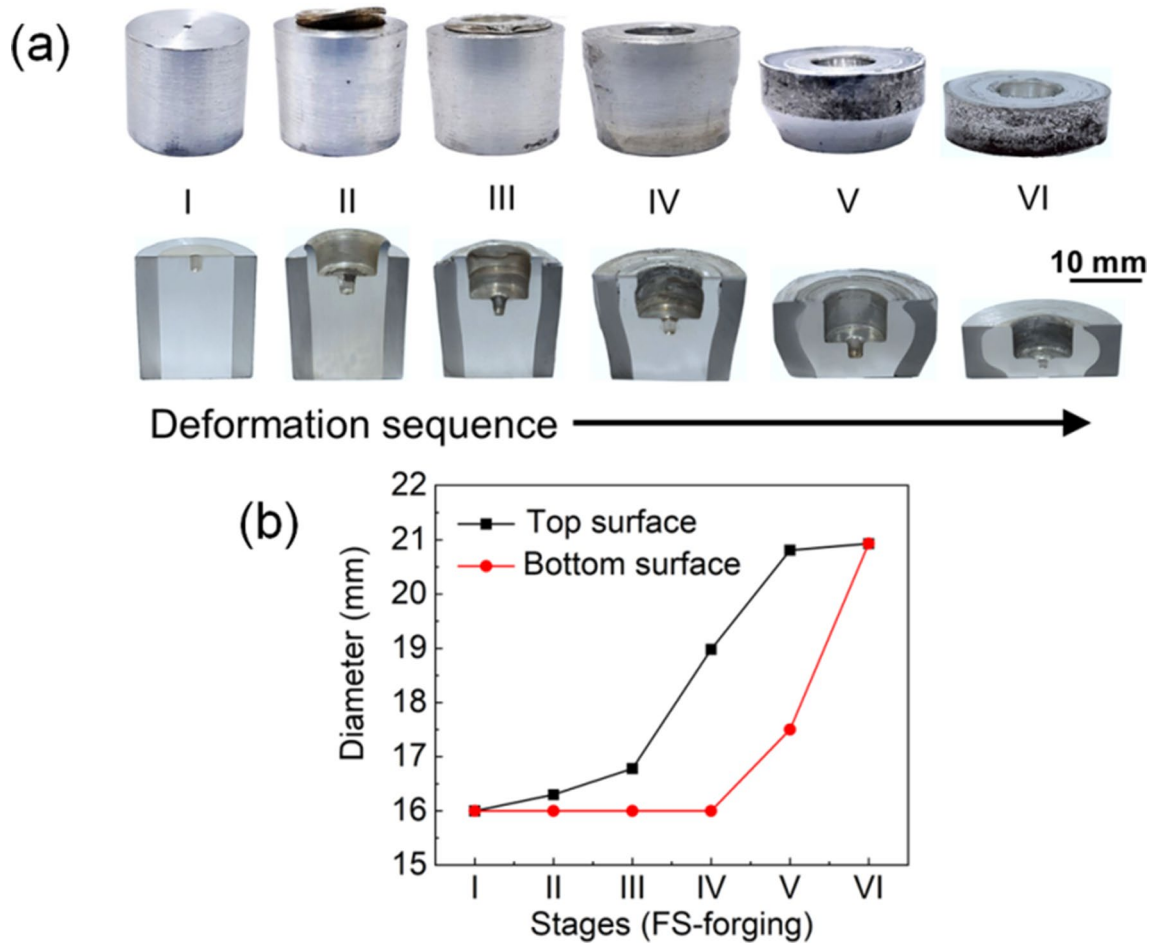**Fig. 3** Force and torque histories of FS-forging

**Fig. 4** Deformation of a Mg/Al blank during FS-forging

Fig. 5 Optical microscopic image of a forged bimetallic blank

(Fig. 6b–g). For the parameter set of 1400/5, the results of EDS line scan across the interface (the region (i) in Fig. 6a) suggest that an intermetallic layer with a thickness of a few tens of µm was developed along the interface, as shown in Fig. 6b, c. The results of point analysis suggest that the greater part of the intermetallic layer is identified as $Al_{12}Mg_{17}$ [16, 17] (p1 in Fig. 6b), while the smaller part of the intermetallic layer near the Al skin has a different chemical composition (p2) of Al_3Mg_2 [18, 19] (Table 3). The point analysis of the dark patches (p3) inside the $Al_{12}Mg_{17}$ intermetallic layer indicates the existence of

unreacted Mg, which suggests an incomplete transformation of Mg to the intermetallic phase. For the thick intermetallic region (ii) in Fig. 6a, the composition of the layer is nearly identical to that obtained from region (i), as shown in Fig. 6d, e, and confirmed by the point analysis of p4. A comparison of the line scan results of regions (i) and (ii) shows that the amount of growth of the $Al_{12}Mg_{17}$ intermetallic layer into the Mg core was much greater than that of the Al_3Mg_2 intermetallic layer into the Al skin.

For the FS-forging with the parameter set of 1400/8, an intermetallic layer with a thickness of a few hundred µm was uniformly developed along the entire interface. The chemical composition of the intermetallic layer is very similar to that from the parameter set 1400/5, as confirmed by the results of the line scan and point analysis (p5) shown in Fig. 6f, g, and Table 3. As expected from the comparison of the results of the regions (i) and (ii) for the process parameter set of 1400/5, most of the growth of intermetallic layer occurred via growth of the $Al_{12}Mg_{17}$ layer into the Mg core. Also, with a longer dwell time of 8 s, i.e., a higher heat input, the unreacted Mg (the

Fig. 6 **a** OM observation on the cross sections of final ring components, **b**, **d**, **f** SEM Images of region i, ii, and iii marked in (**a**), **c**, **e**, **g** corresponding element line-scanning spectrums
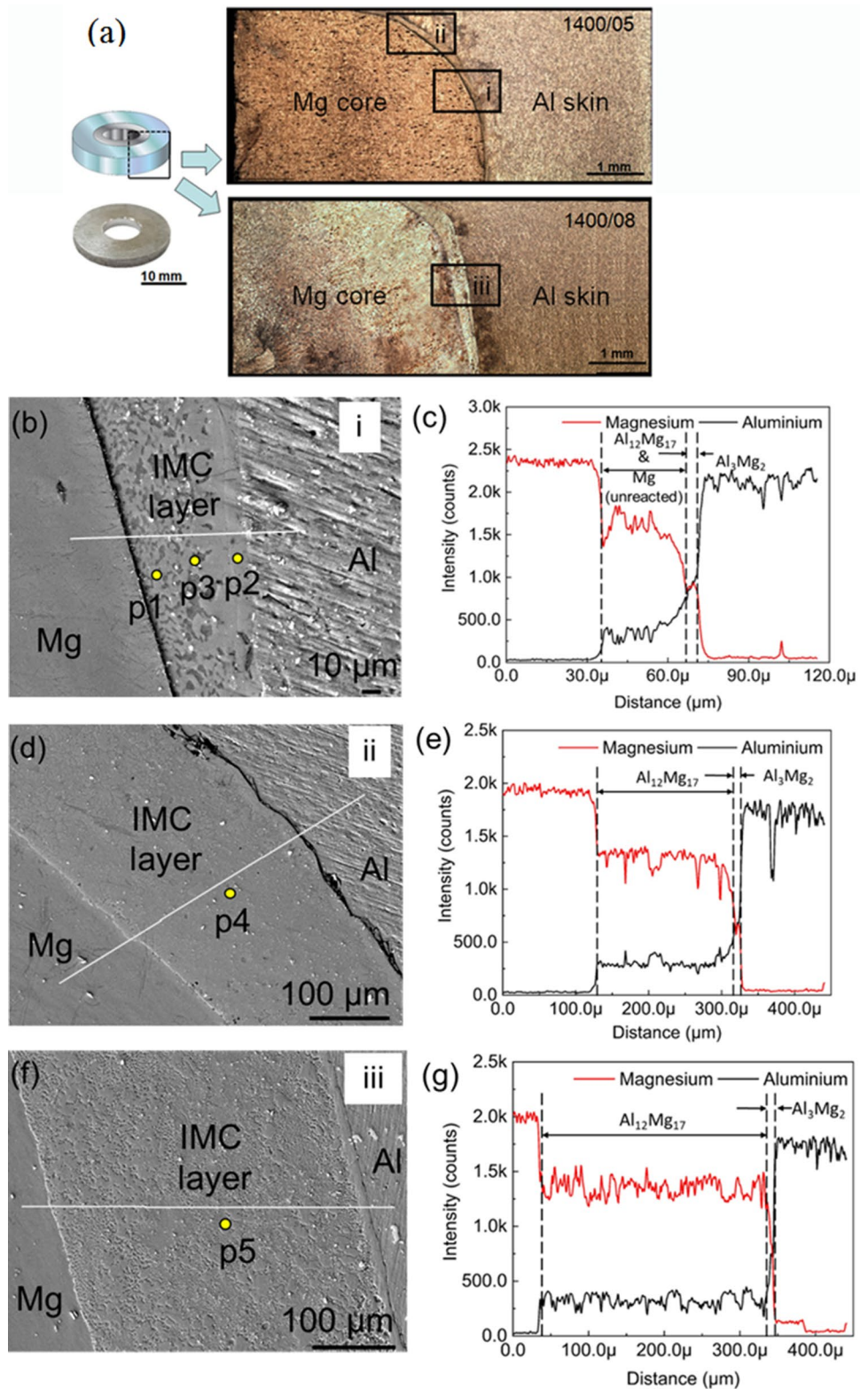
dark patches) observed in Fig. 6b for the dwell time of 5 s disappeared.

The inverse pole figure (IPF) maps for hoop direction (HD) from EBSD analysis for the base Mg core and Al skin display typical microstructures after extrusion at elevated temperatures (especially for the Mg core), as shown in Fig. 7. The vertical direction is the extruded direction, whereas the thickness represents the transverse direction.

Table 3 Chemical composition at different positions in Fig. 6b, d, and f

Parameter set	Regions	Points	Mg (at.%)	Al (at.%)
1400/05	i	p1	66.04	33.96
		p2	40.73	59.27
		p3	83.69	16.31
	ii	p4	67.93	32.07
1400/08	iii	p5	63.71	36.29

The kernel average misorientation (KAM) maps show grains with low dislocation density due to recrystallization and/or recovery in both the base Mg core and Al skin (blue regions).

The EBSD analysis shows that the microstructures of the Mg core and Al skin were differently affected by the FS-forging, depending on the location within the bimetallic blank, as shown in Fig. 8 for the process parameter set of 1400/8. The Mg core shows a refined microstructure without large grains observed in the base metal, as a result of dynamic recrystallization (DRX) induced by friction stirring of the rotating tool. The extent of grain refinement along the radial direction becomes more significant into the Mg core. This indicates that the grains closer to the inner surface of the ring component were more severely friction stirred by the tool. Near the interface of the Mg core and Al skin, the Mg core shows an almost random texture with a slight grain growth.

On the contrary, the microstructure of the Al skin shows a deformed microstructure with a decreased average grain size compared to the base Al skin. The decreased average grain size suggests that some extent of DRX still occurred, even though it was less than that which occurred on the Mg core side. The abrupt change in the microstructural trend across the interface suggests that friction stirring of material much more severely occurred inside the Mg core, while the Al skin was mostly deformed by the radial expansion of the Mg core at the elevated temperature. This is confirmed by the clean interface between the Mg core and the Al skin observed in the cross sections of the FS-forged rings in Fig. 6a. If friction stirring had also dominated the deformation of Al skin, the clean interface between the Mg core and the Al skin would have not been obtained due to intermixing of the two

Grain size: 11.0 ± 8.7 μm

Magnesium

Grain size: 66.8 ± 26.5 μm

Aluminum
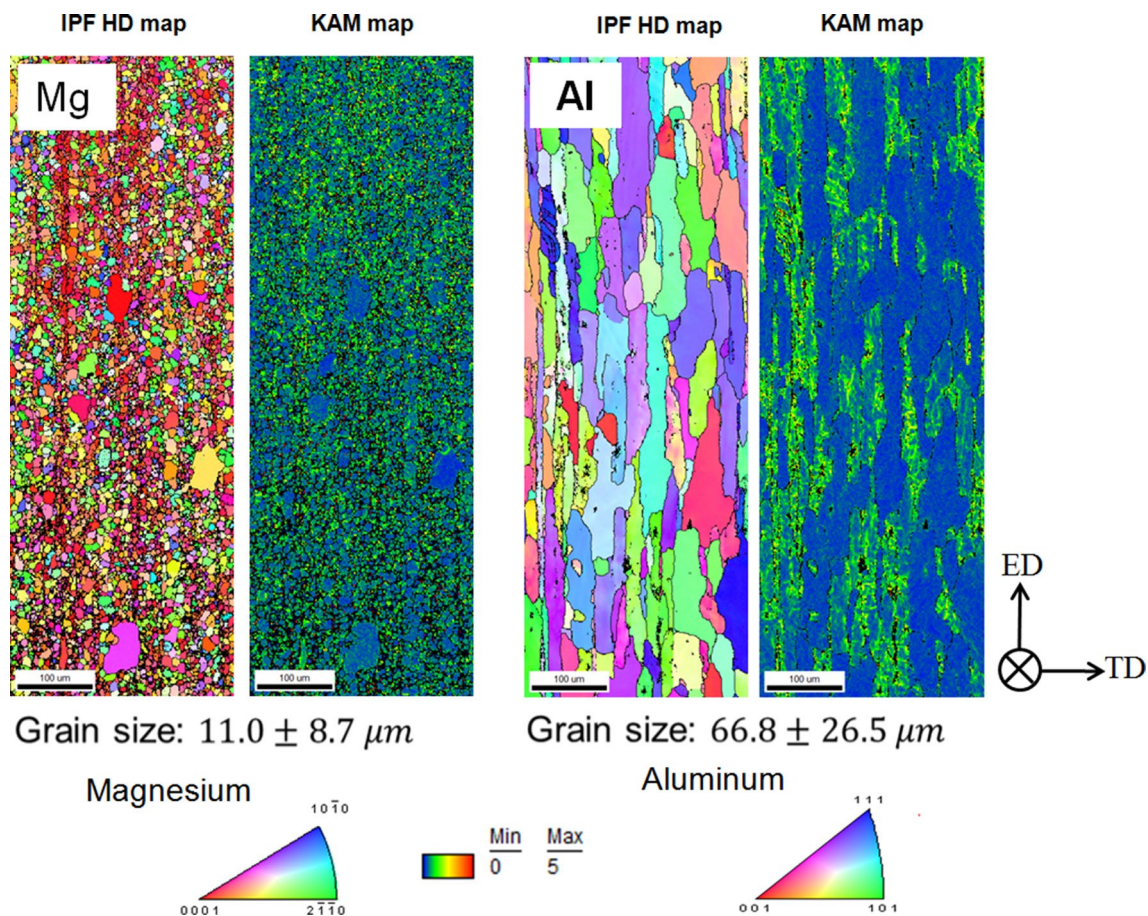
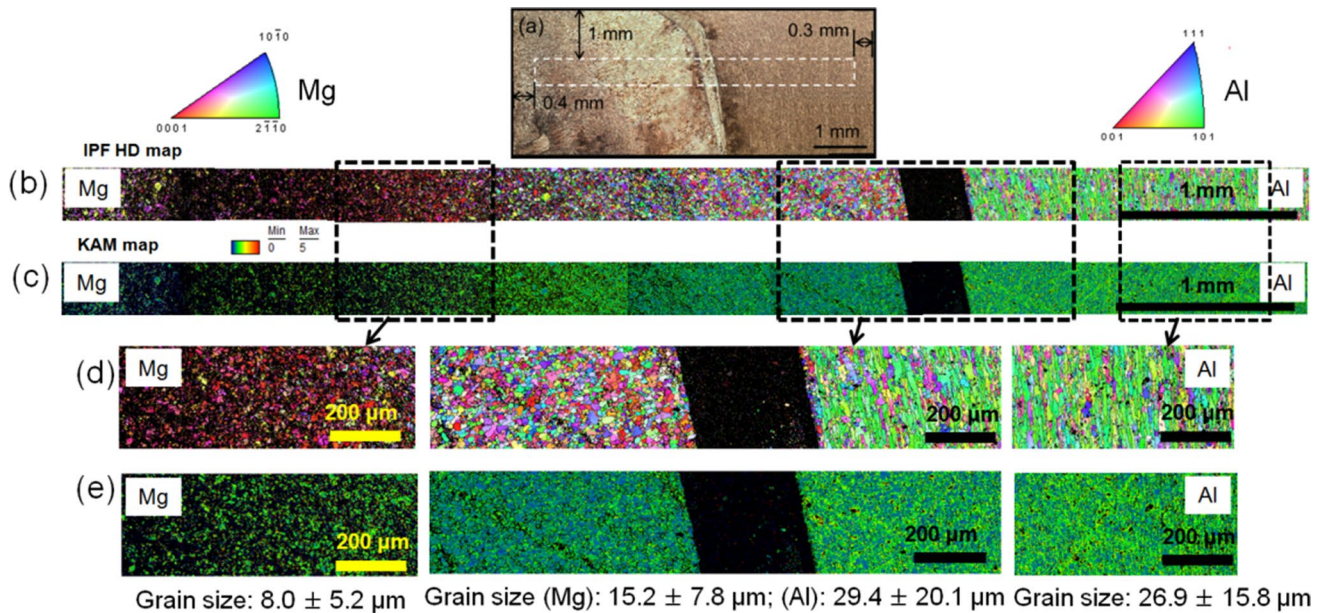**Fig. 7** EBSD analysis of base metals: IPF and KAM maps

Fig. 8 EBSD analysis of FS-forged Mg/Al bimetallic ring with the parameter set 1400/8: **a** cross section; **b** IPF and **c** KAM of the white box region; **d**, **e** magnified images of the areas of the Mg core, Al skin, and their interface marked by black boxes in (**b**, **c**)

dissimilar alloys. Instead, intermixing of the two dissimilar alloys would have induced complicated ring structures, as typically observed in conventional friction stir spot welding [20].

Note that the IPF and KAM maps of the intermetallic layer could not be obtained as the intermetallic phases in the layer could not be indexed. It was unable to obtain the Kikuchi pattern for the layer. The EBSD analysis for the process parameter set of 1400/5 shows quite similar results of grain refinement and will not be presented here.

For the parameter sets in the present study, the hardness profiles in the radial direction at the middle of the cross section were similar (Fig. 9). The fluctuating hardness value inside the Mg core represents the variation of the extent of DRX and resultant microstructures. The hardness values of the intermetallic layer were significantly higher than those of the Mg core and Al skin, which corresponds well to the material characteristics of the Mg/Al intermetallics [16, 21]. The width of the high hardness regions for 1400/5 and 1400/8 parameter sets also correspond well to the thickness of the intermetallic layers, as observed in SEM analysis across the joint interface.

4 Conclusion

The FS-forging, which is a friction stir assisted simultaneous forging and solid-state joining process, was suggested. The feasibility of the process was successfully confirmed by fabricating a Mg/Al bimetallic ring component. The process
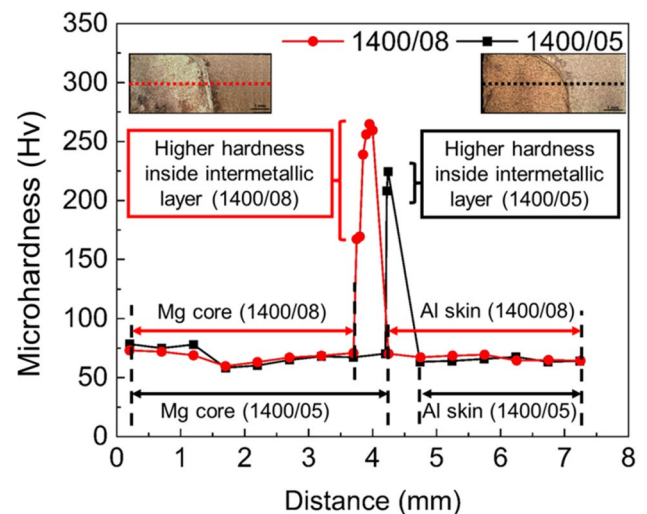

Fig. 9 Hardness profiles along middle of the cross-section in the radial direction for two different sets of parameters

eliminated the requirement of external heating by applying friction heat using a rapidly rotating tool, which also served as a part of forming die. The frictional heat and plastic flow induced by the rotation and plunging of the tool provided an ideal condition for diffusion bonding along the interface of the Mg core and Al skin, which induced intermetallic phases along the interface. While the feasibility of the suggested process was successfully demonstrated by selecting a well-known brittle Mg alloy as one of the materials for simultaneous forging and joining in the present study, the

concept of FS-forging can be easily extended to different dissimilar material combinations for the manufacture of various structural or electric components.

Compliance with ethical standards

Conflict of interest On behalf of all authors, the corresponding author states that there is no conflict of interest.

References

1. Fan S, Jiang W, Li G, Mo J, Fan Z (2017) Fabrication and microstructure evolution of al/mg bimetal using a near-net forming process. Mater Manuf Process 32(12):1391–1397
2. Bae JH, Rao AKP, Kim KH, Kim NJ (2011) Cladding of mg alloy with al by twin-roll casting. Scripta Mater 64(9):836–839
3. Golovko O, Bieliaiev SM, Nürnberger F, Danchenko VM (2015) Extrusion of the bimetallic aluminum-magnesium rods and tubes. Forsch Ingenieurwes 79:17–27
4. Ng M-K, Li L, Fan Z, Gao RX, Smith EF III, Ehmann KF, Cao J (2015) Joining sheet metals by electrically-assisted roll bonding. CIRP Ann Manuf Technol 64(1):273–276
5. Napierala O, Dahnke C, Tekkaya AE (2019) Simultaneous deep drawing and cold forging of multi-material components: draw-forging. CIRP Ann Manuf Technol 68(1):269–272
6. Evans WT, Gibson BT, Reynolds JT, Strauss AM, George EC (2015) Friction stir extrusion: a new process for joining dissimilar materials. Manuf Lett 5:25–28
7. Buffa G, Baffari D, Ingarao G, Fratini L (2020) Uncovering technological and environmental potentials of aluminum alloy scraps recycling through friction stir consolidation. Int J Precis Eng Manuf Green Tech. https://doi.org/10.1007/s40684-019-00159-5
8. Das H, Mondal M, Hong S-T, Chun D-M, Han HN (2018) Joining and fabrication of metal matrix composites by friction stir welding/processing. Int J Precis Eng Manuf Green Tech 5:151–172
9. Allwood JM, Kopp R, Michels D, Music O, Öztop M, Stanistreet TF et al (2005) The technical and commercial potential of an incremental ring rolling process. CIRP Ann Manuf Technol 54(1):233–236
10. Shivpuri R (1988) Past developments and future trends in the rotary or orbital forging process. J Mater Shaping Technol 6(1):55–71
11. Luo W, Chen F, Xu B, Yang Z, Guo Y et al (2018) Study on compound spinning technology of large thin-walled parts with ring inner ribs and curvilinear generatrix. Int J Adv Manuf Technol 98:1199–1216
12. Cleaver CJ, Arthington MR, Mortazavi S, Allwood JM (2016) Ring rolling with variable wall thickness. CIRP Ann Manuf Technol 65(1):281–284
13. Whalen S, Overman N, Joshi V, Varga T, Graff D et al (2019) Magnesium alloy zk60 tubing made by shear assisted processing and extrusion (ShAPE). Mater Sci Eng A 755:278–288
14. Tokunaga T, Szeliga D, Matsuura K, Ohno M, Pietrzyk M (2015) Sensitivity analysis for thickness uniformity of al coating layer in extrusion of mg/al clad bar. Int J Adv Manuf Technol 80:507–513
15. Hong S-T, Mondal M, Zhang S, Gao K, Das H, Han HN, Park J-W, Jeong H-J (2019) Friction stir forging apparatus and method. KR Patent, 10-2041853
16. Zhu B, Liang W, Li X (2011) Interfacial microstructure, bonding strength and fracture of magnesium–aluminum laminated composite plates fabricated by direct hot pressing. Mater Sci Eng A 528:6584–6588
17. Suhuddin U, Fischer V, Kroeff F, Santos JFD (2014) Microstructure and mechanical properties of friction spot welds of dissimilar AA5754 Al and AZ31 Mg alloys. Mater Sci Eng A 590:384–389
18. Kostka A, Coelho RS, Santos JD, Pyzallac AR (2009) Microstructure of friction stir welding of aluminium alloy to magnesium alloy. Scripta Mater 60:953–956
19. Suhuddin U, Fischer V, Santos JFD (2013) The thermal cycle during the dissimilar friction spot welding of aluminum and magnesium alloy. Scripta Mater 68:87–90
20. Hong S-T, Das H, Oh HS, Al Nasim MNEA, Chun D-M (2017) Combination of nano-particle deposition system and friction stir spot welding for fabrication of carbon/aluminum metal matrix composite joints of dissimilar aluminum alloys. CIRP Ann Manuf Technol 66(1):261–264
21. Dietrich D, Nickel D, Krause M, Lampke T, Coleman MP, Randle V (2011) Formation of intermetallic phases in diffusion-welded joints of aluminium and magnesium alloys. J Mater Sci 46:357–364

Mounarik Mondal Ph.D. candidate in the School of Mechanical Engineering, University of Ulsan. His research interests are friction stir welding and processing.

Soumyabrata Basak Ph.D. candidate in the School of Mechanical Engineering, University of Ulsan. His research interests are friction stir welding and processing.

Hrishikesh Das Post-Doctoral Research Associate in the Applied Materials and Manufacturing Group, at the Pacific Northwest National Laboratory, United States. He was previously with Mechanical Engineering Department, University of Ulsan, South Korea as a Post-Doctoral Researcher. His research interests include friction-stir welding and solid phase processing.

Ju-Won Park Ph.D. in Department of Materials Science & Engineering, Seoul National University. His research interest is electro-treatment and microstructure for materials.

Sung-Tae Hong Professor in the School of Mechanical Engineering at the University of Ulsan, South Korea. His research interests include metal forming, electrically assisted manufacturing, and solid state joining.

Heung Nam Han Professor in Department of Materials Science and Engineering, Seoul National University. His research interest is the mechanical behaviour and microstructure characterization for materials.

Howook Choi Ph.D. candidate in Department of Materials Science & Engineering, Seoul National University. His research interest is electro-treatment and electrically assisted processing for metallic materials.